Journal of Applied Sciences

ISSN 1812-5654

Journal of Applied Sciences 14 (2): 144-150, 2014
ISSN 1812-5654 / DOI: 10.3923/jas.2014.144.150

Research of the Constant Current Characteristic of Symmetric AC-AC Inductive Coupled Power Transfer System

Lu Zhang, Yue Sun, Zhihui Wang and Chunsen Tang
College of Automation, Chongqing University, 400030, Chongqing, China

Abstract: This study proposes a novel symmetric AC-AC converter for Inductive Power Transfer (ICPT) system which has simple and symmetric circuit topology without requiring large filter capacitor and rectifier. It takes 50 Hz sinusoidal mains input and generates 50 Hz sinusoidal mains output. The constant current characteristic of the system is verified by theoretical analysis based on impulse theorem. The parameter of the resonant link is also derived to ensure the frequency stability of system. Preliminary Simulation and experimental results have verified the validity of the system.

Key words: AC-AC, inductive coupled power transfer, constant current characteristic, impulse theorem

INTRODUCTION

Inductively coupled power transfer (ICPT) technology allows electrical energy to be transferred from a stationary primary source to one or more movable secondary loads over relatively large air gaps (Si *et al*., 2008; Li *et al*., 2008). Due to the elimination of physical electric contacts, it is widely used in special fields, such as inflammable and explosive areas and wet or undersea environment (Sample *et al*., 2011; Li *et al*., 2012a, 2013; Dai and Sun, 2011; Tang *et al*., 2009). Moreover, in most industrial ICPT applications, only ac mains are available, so several research have been done to achieve AC output (Boys *et al*., 2008; Keeling *et al*., 2010; Sun *et al*., 2012).

Normally, in order to generate a high-frequency current on the primary side, an AC-DC-AC two-stage power conversion is employed in ICPT systems (Wang *et al*., 2010, 2011). However, extra semiconductor switches and large DC electrolytic capacitors can be costly and bulky (Safaee *et al*., 2012; Wu *et al*., 2011a) which also compromises system reliability. Meanwhile, for high power application, power factor correction circuitry is usually employed along with the rectification stage.

Recently, one of the options to design a direct AC-AC ICPT system is to generate a high-frequency current on the primary side based on free oscillation and energy injection control (Li *et al*., 2012b). The converter is simplicity but neglect the envelop characteristic of the track current and the design of the pickup. Moreover, it has been pointed out that a low energy storage power supply can be used to achieve AC-AC conversion (Wu *et al*., 2011b). Such technique can directly generate high frequency track currents whereas the AC-DC stage is still used because that such technique needs a small filter capacitor after the rectifier to reduce the energy storage of the power supply.

In this study, a novel direct sinusoidal input/output AC-AC ICPT system is presented without energy storage links. Compared with the traditional AC-DC-AC ICPT system, its structure and control are simple and the cost is lower. This technique combines the primary direct AC-AC converter with a secondary AC-AC converter based on energy injection control that converts the high frequency AC directly to a low frequency AC output. The expression for the steady load current based on impulse theorem has been discussed in detail. Simulations and experiments have been carried out to verify the theoretical results.

BASIC CIRCUIT OPERATION

The ICPT system can be classified by voltage-fed system and current-fed system. The voltage-fed system normally matches series tuned types of resonant tanks, while current-fed system matches parallel tuned types of resonant tanks. This study uses a typical voltage-fed resonant tank as an example. The main AC-AC topology of voltage-fed ICPT system can be shown in Fig. 1.

As shown in Fig. 1, the system has the symmetric circuit topology from primary part to secondary part. The series resonant network of the primary part consisting of a capacitor C_p in series with an inductor L_p, such series resonant tank is assumed to be driven to produce a high-frequency sinusoidal current with low distortion directly from input AC supply. This sinusoidal current provide the Zero Current Switching (ZCS) conditions for IGBT switches (P_1~P_4).

Corresponding Author: Lu Zhang, College of Automation, Chongqing University, 400030, Chongqing, China

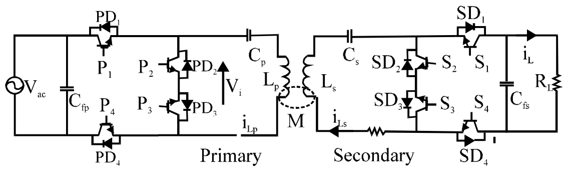

Fig. 1: Symmetric AC-AC voltage-fed ICPT system

The secondary part consists the pick up coil L_s which is completely tuned by the series capacitor C_s and the M is the mutual inductance between L_p and L_s, such series resonant tank receives the high-frequency energy by the magnetic fields coupling. The symmetric AC-AC converter that includes four switches (S_1~S_4) converts the induced high frequency AC directly to a low frequency AC output to the load R_L.

Primary AC-AC converter operation (the energy injection and free oscillation control method): The four IGBTs (P_1~P_4) and four anti-parallel diodes (PD_1~PD_4) constitute two pairs bidirectional switch to convert the input AC supply into a series of the high frequency rectangular voltage waveform whose amplitude changed according to sinusoidal law (Fig. 2). The primary AC-AC converter operate based on energy injection mode and free oscillation mode: When the polarity of the input AC supply and the resonant current is positive, P_1 switched "on", while other switches (P_2~P_4) be "off" and the energy is injected into the primary resonant tank, as the polarity of resonant current is negative then P_2 switched "on", while other switches (P_1, P_3, P_4) be "off" and the energy free oscillate in the resonant tank. The signals and waves corresponding to the principle are seen as Fig. 2.

Impulse theorem: There is a very important conclusion called impulse theorem in sample control theory which is the narrow pulses of equal impulse and different shape have the same effect when added to the inertia link. Impulse is the area of narrow pulses and the same effect means to get the same output response wave (Zheng *et al*., 2010).

Based on the impulse theorem (also called equivalent area principle), in order to make the output voltage waveform equivalent with the desired voltage waveform, the area sum of surrounded by sinusoid half wave with power grid frequency within the half output voltage period must be equal to the one of desired output voltage wave. It especially needs to be pointed that the wave of sinusoid half wave of the input supply is chopped by high frequency pulse signals based on energy injection and free oscillation principal (Fig. 3).

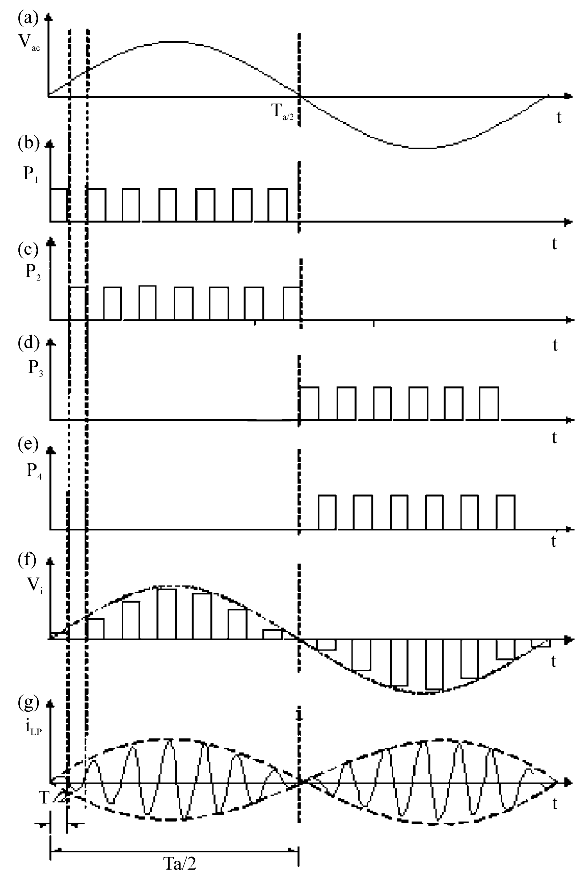

Fig. 2(a-g): Control sequence of the AC-AC resonant soft-switched converter of primary part, (a) Input voltage waveform, (b) Control pulse waveform of P_1, (c) Control pulse waveform of P_2, (d) Control pulse waveform of P_3, (e) Control pulse waveform of P_4, (f) Output voltage waveform of the primary inverter and (g) Resonant current waveform of the L_P

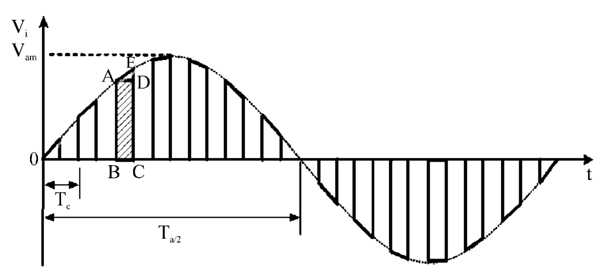

Fig. 3: Output voltage waveform of primary AC-AC inverter

From Fig. 3, let the amplitude of the input AC supply be V_{am}, frequency be f_a, period be T_a, then the voltage waveform of the input AC supply can be expressed as follow:

$$V_{ac} = V_{am} \sin 2\pi f_a t \tag{1}$$

In order to facilitate analysis of the circuit and highlight the main issues, supposed the resonant frequency f_c is large enough, then the area of each trapezoidal curve (S_{ABCE}) can be replaced by the rectangle area (S_{ABCD}), then each area of the voltage S_j can be expressed as:

$$S_j = 0.5T_c V_i(j) \tag{2}$$

where, $V_i(j)$ is the length of the rectangle (S_{ABCD}) that is replaced by the instantaneous voltage (t = j) and the width of the rectangle is the half resonant period ($0.5T_c$). The zero phase frequency must be equal to the secondary resonant frequency so that the maximum output power could be achieved (Wang *et al*., 2004). Therefore, the resonant period T_c should be:

$$T_c = \frac{1}{f_c} = \frac{2\pi}{\omega_0} = 2\pi\sqrt{L_p C_p} = 2\pi\sqrt{L_s C_s} \tag{3}$$

where, the ω_0 is the zero phase angular frequency of the system, as shown in Fig. 3, the area of surrounded by every sinusoid half wave with the input power after inverted by the high frequency control pulse (S) is expressed as follow:

$$S = \sum_{j=1}^{N} S_j = \frac{V_{am}}{2f_c}\sum_{j=1}^{N}\sin 2\pi f_a(j-0.5)\frac{1}{f_c} \tag{4}$$

where, the N is:

$$N = \frac{0.5T_a}{T_c} = 0.5\frac{f_c}{f_a} \tag{5}$$

Then the voltage injected into the primary resonant tank should be:

$$V = \frac{\sum_{j=1}^{N} S_j}{0.5T_a} = \frac{f_a V_{am}}{f_c}\sum_{j=1}^{N}\sin 2\pi f_a(j-0.5)\frac{1}{f_c} \tag{6}$$

The resonant current of primary part i_{Lp} can be derived as:

$$i_{L_p} = \frac{V}{R_r} = \frac{\frac{f_a V_{am}}{f_c}\sum_{j=1}^{N}\sin 2\pi f_a(j-0.5)\frac{1}{f_c}}{R_r} \tag{7}$$

where the reflected impedance R_r that is dependent on the transformer coupling and operating frequency is given by:

$$R_r = \frac{\omega_0^2 M^2}{Z_s} \tag{8}$$

where, Z_s is the impedance of the secondary part and M is the mutual inductance between primary coil and secondary coil.

Secondary AC-AC converter operation: Similarly, the working principle of the secondary part is also based on the energy injection and free oscillation mode, it is the inverse process of the primary part. The high frequency resonant current induced from the primary part is converted into low frequency current waveform whose amplitude changed according to sinusoidal law, the signals and waves corresponding to above principle are seen as Fig. 4.

The equivalent circuit of the secondary part based on the mutual induction model is shown in Fig. 5.

According to the AC impedance model of system resonant tank, the induced voltage V_{oc} of the secondary resonant inductance L_s can be:

$$V_{oc} = \omega_0 M i_{Lp} \tag{9}$$

Then, the current of the secondary inductance i_{Ls} should be :

$$i_{Ls} = \frac{V_{oc}}{Z_s} = \frac{V_{oc}}{j\omega L_s + \frac{1}{j\omega C_s} + R_s + R_{eq}} \tag{10}$$

where, R_{eq} is the equivalent resistance of the output port of the secondary resonant link and R_s is the inherent resistance of inductor L_s. Substituting Eq.7-9 into Eq.10, the secondary inductance current i_{Ls} is derived as:

$$i_{Ls} = \frac{V}{\omega_0 M} = \frac{f_a V_{am}}{\omega_0 M f_c}\sum_{j=1}^{N}\sin 2\pi f_a(j-0.5)\frac{1}{f_c} \tag{11}$$

It can be seen from Eq.11 that the i_{Ls} is independent of the load R_L, in addition, the on-and-off period of the switch S_L is equal, suppose the working time of the circuit is σ, the expression of the equation as follow can be given according to energy conservation principle:

$$I_{LS}^2 R_{eq}\sigma = I_{LS}^2 R_L \frac{\sigma}{2} = I_L^2 R_L \sigma \tag{12}$$

Then substituting Eq.12 into Eq.11, the load current i_L can be obtained as follow:

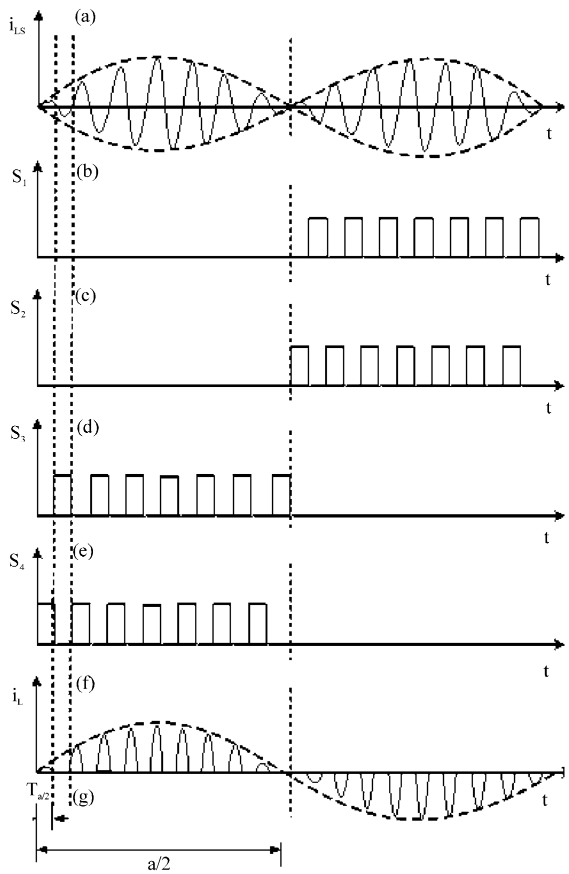

Fig. 4(a-g): Control sequence of the AC-AC resonant soft-switched converter of secondary part, (a) Resonant current waveform of the L_S, (b) Control pulse waveform of S_1, (c) Control pulse waveform of S_2, (d) Control pulse waveform of S_3, (e) Control pulse waveform of S_4, (f) Output voltage waveform of the primary inverter and (g) Load current waveform of the secondary

$$i_L = \frac{i_{LS}}{\sqrt{2}} = \frac{\sqrt{2} f_a V_{am}}{2\omega_0 M f_c} \sum_{j=1}^{N} \sin 2\pi f_a (j-0.5) \frac{1}{f_c} \tag{13}$$

From Eq.13, it can been obviously seen that the load current i_L is completely independent of the load R_L, in other words, the system exactly has the constant current characteristic.

Frequency stability: Form Eq. 13, it can be seen that the constant current characteristic of the system depend on the resonant frequency f_c. In order to ensure there is only one zero phase angle frequency, parameters of the system should be satisfied as follow (Zhang *et al*., 2013):

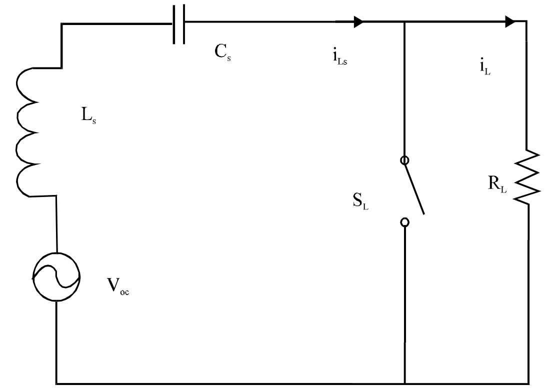

Fig. 5: Equivalent circuit diagram of the AC-AC resonant soft-switched converter of secondary part

$$\begin{cases} 0 < R_L < (\sqrt{2}\omega_0 L_s - R_s)/2, & k \in \left[0, \sqrt{\Gamma}\right) \\ R_L \ge (\sqrt{2}\omega_0 L_s - R_s)/2, & k \in [0,1] \end{cases} \tag{14}$$

where the expression of the coupling coefficient *k* is given by:

$$k = M\big/\sqrt{L_p L_s} \qquad k \in [0,1] \tag{15}$$

The M is the mutual inductance between primary coil and secondary coil. In addition the Γ is defined as shown below:

$$\Gamma = \frac{4\omega_0^2 L_s^2 (R_{eq} + R_s)^2 - (R_{eq} + R_s)^4}{4\omega_0^4 L_s^4} \tag{16}$$

SIMULATION AND EXPERIMENTAL RESULTS

Simulation analysis: On the basis of the analysis discussed above, the simulation model in MATLAB/SIMULINK software of the proposed AC-AC ICPT system can be easily built with the parameters shown in Table 1.

The simulation waveforms of the system are as shown in Fig. 6 and 7. It can be seen from Fig. 6b that the primary resonant current i_{Lp} can be directly generated by the input AC supply that is shown in Fig. 6a. The steady-state waveform is achieved after 5 msec and the envelope of the resonant current is in good quality by using the energy injection and free oscillation control method, the current amplitude of i_{Lp} is 20 A. The enlarged drawing of the resonant current (39.5~40.5 msec) shown as Fig. 6c shows that the frequency of current i_{Lp} is 20 kHz and made to be a low distortion sinusoidal shape, the system operates at ZCS condition because the control pulse waveform of P_1 is in phase with i_{Lp}.

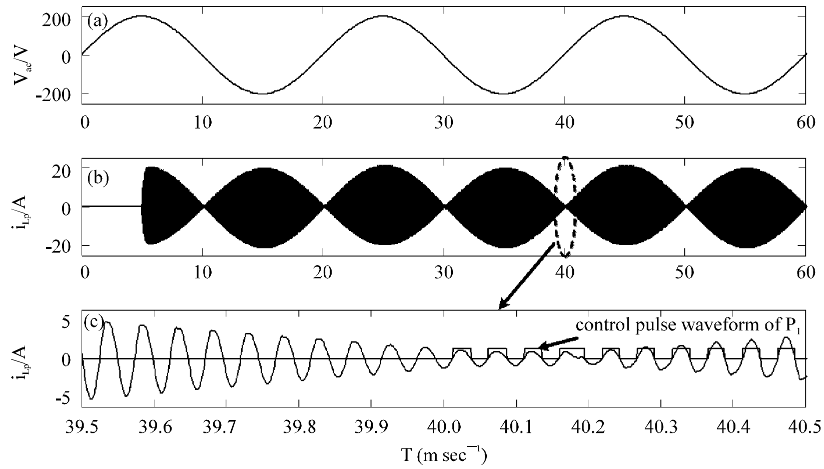

Fig. 6(a-c): Input AC voltage, resonant current and control pulse waveform of primary part, (a) Primary input ac supply, (b) Resonant current and (c) Enlarged drawing of the resonant current

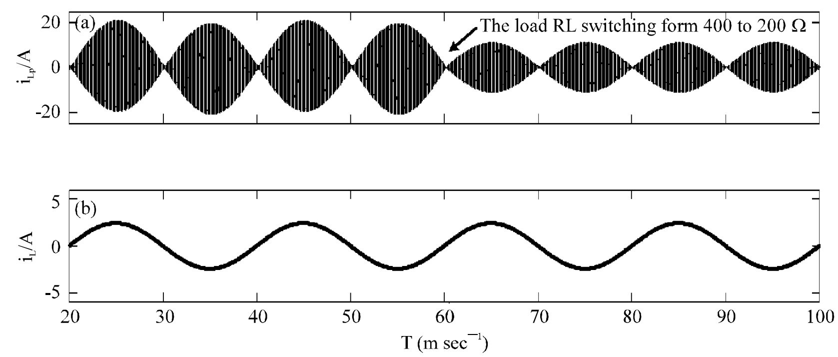

Fig. 7(a-b): Resonant current waveform of primary part and load

Table 1: Parameters of proposed AC-AC ICPT system

Parameters	Values
Input AC supply magnitude V_{am}(V)	200.00
Supply frequency f_a (Hz)	50.00
Primary capacitance filter C_{fp}(µF)	1.00
Secondary capacitance filter C_{fs}(µF)	1.00
Nominal resonant frequency f_0 (kHz)	20.00
Primary resonant inductance L_p (µH)	423.00
Primary resonant capacitance C_p (µF)	0.15
Secondary resonant inductance L_s (µH)	423.00
Secondary resonant capacitance C_s (µF)	0.15
Mutual inductance M (µH)	150.00
Resistance of secondary inductor R_s (Ω)	0.10
Resistance of the load R_{L1} (Ω)	400.00
Resistance of the load R_{L2} (Ω)	200.00
AC input load current i_L (A)	2.00

The resonant current waveform of primary part and load current waveform of secondary part with dynamic load switching is shown as Fig. 7.

Current waveform of secondary part with dynamic load switching (a) Primary resonant current waveform with the load R_{L1} = 400 Ω varying from R_{L2} = 200 Ω and (b) Load current waveform with the load R_{L1} = 400 Ω varying from R_{L2} = 200 Ω.

From Fig. 7a, as the load R_L varies from R_{L1} = 400 Ω to R_{L2} = 200 Ω the primary resonant current i_{Lp} varies from 20 to 10 A, simultaneously, the load current i_L shown as Fig. 7b keeps at 2 A, this proves that the symmetric AC-AC ICPT system exactly has the constant current characteristic.

It also can be seen from Fig. 7b that the load current i_L is 50 Hz and made in good quality by the low-pass filtering tank followed of the inverter.

DISCUSSION

The symmetric AC-AC ICPT system shown in Fig. 1 has been implemented in a laboratory scale. The inverter consists of four IGBTs (International Rectifier IRGBC40K). The zero-crossing points of inductance current are detected by the current sense transformers

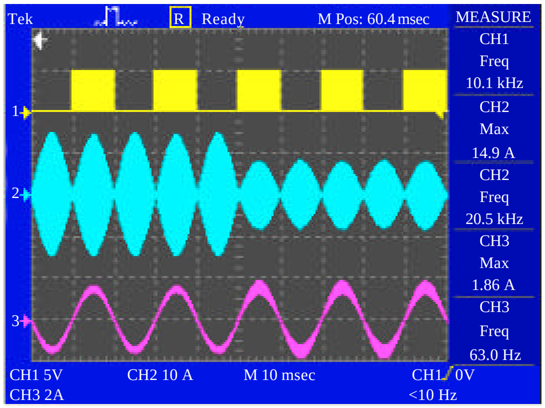

Fig. 8: Experimental waveforms of proposed symmetric AC-AC ICPT system with the load R_{L1} = 400 Ω varying from R_{L2} = 200 Ω. (CH1: Control pulse of P_1-5 V/div; CH2: Current of the primary inductor i_{Lp}-10 A/div; CH3: Current of the load i_L-2 A/div)

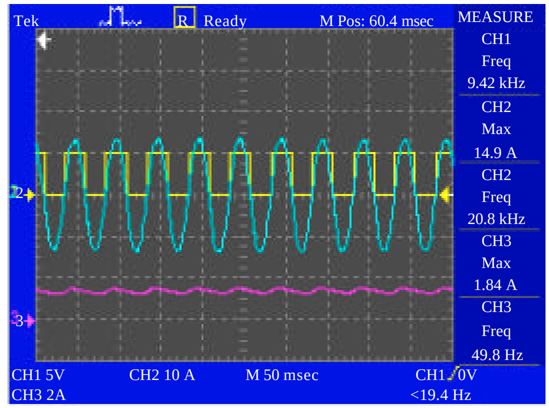

Fig. 9: Steady-state experimental waveforms of the resonant current and control pulse of primary part (CH1: Control pulse of P_1-5 V/div; CH2: Current of the primary inductor i_{Lp}-10 A/div; CH3: Current of the load i_L-2 A/div)

(Talema AS-103). Phase-locked loop (CD4046) is selected to achieve the ZCS operation for the converter with variable frequency. According to the parameters in Table 1. The experimental results of the proposed ICPT system are shown below.

Figure 8 shows the experimental waveforms the symmetric AC-AC ICPT system, the primary resonant current i_{Lp} is controlled based on the energy injection and free oscillation mode, it can be seen from Fig. 8 that the peak resonant current i_{Lp} decrease from 8 to 14.9 A as the load R_L is switched from 400 to 200 Ω, while the amplitude of the output load current i_L still remains at 1.86 A and the frequency keeps at 49.8 Hz. Considering the coil resistance and conduction loss in actual system, the experimental results are lower than the simulation value which is obtained under ideal situation. In addition, the load current i_L shown in Fig. 8 (CH3) has slight ripple which is caused by the output filter capacitor C_{fs} whose discharge time is affected by the sudden change of the load resistance. However, compared with the fact that the power of the system decreased by 50% under dynamic load switching condition, such slight current ripple will not affect our conclusion that the system does have the constant current characteristic.

From Fig. 9, it can be seen that the system has achieved ZCS as the resonant current i_{Lp} is in phase with control pulse of P_1. It also can be seen that the experimental curve of the current i_{Lp} deviates of by about 0.8 kHz from the theoretical value. This is caused by deviations in actual component values from the nominal values. The theoretical results are based on the simplifications in the model that ignores losses in the capacitors and electromagnetic structure. Therefore, this error in practice doesn't affect the analyzed results above this section.

CONCLUSION

This study put forward a symmetric AC-AC ICPT system without requiring energy storage links. The expression for the steady load current based on impulse theorem has been discussed in detail under dynamic load switching condition. Simulations and experiments have been carried out to validate the constant current characteristic of the system and it realizes 50 Hz sinusoidal mains input and generates 50 Hz sinusoidal mains output without any large filter capacitor and rectifier, this could save cost and volume of the ICPT system and the system complexity is also been reduced.

ACKNOWLEDGMENTS

This study is financially supported by National Natural Science Foundation of China (No. 51207173, 51277192). I also would like to give my special thanks to the anonymous reviewers for their contributions to this study.

REFERENCES

Boys, J.T., C.Y. Huang and G.A. Covic, 2008. Single-phase unity power-factor inductive power transfer system. Proceedings of the IEEE Power Electronics Specialists Conference, June 15-19, 2008, Rhodes, Greece, pp: 3701-3706.

Dai, X. and Y. Sun, 2011. Study on energy injection control method for inductive power transfer system. J. Univ. Electron. Sci. Technol. China, 40: 69-72.

Keeling, N.A., G.A. Covic and J.T. Boys, 2010. A unity-power-factor IPT pickup for high-power applications. IEEE Trans. Ind. Electron., 57: 744-751.

Li, H.L., A.P. Hu and G.A. Covic, 2008. FPGA controlled high frequency resonant converter for contactless power transfer. Proceedings of the IEEE Power Electronics Specialists Conference, June 15-19, 2008, Rhodes, Greece, pp: 3642-3647.

Li, H.L., A.P. Hu and G.A. Covic, 2012a. A direct AC-AC converter for inductive power-transfer systems. IEEE Trans. Power Electron., 27: 661-668.

Li, Y.L., Y. Sun and X. Dai, 2012b. Controller design for an uncertain contactless power transfer system. Inform. Technol. J., 11: 971-979.

Li, Y.L., Y. Sun and X. Dai, 2013. i-Synthesis for frequency uncertainty of the ICPT system. IEEE Trans. Ind. Electron., 60: 291-300.

Safaee, A., D. Yazdani, A. Bakhshai and P.K. Jain, 2012. Multiblock soft-switched bidirectional AC-AC converter using a single loss-less active snubber block. IEEE Trans. Power Electron., 27: 2260-2272.

Sample, A.P., D.A. Meyer and J.R. Smith, 2011. Analysis, experimental results and range adaptation of magnetically coupled resonators for wireless power transfer. IEEE Trans. Ind. Electron., 58: 544-554.

Si, P., A.P. Hu, S. Malpas and D. Budgett, 2008. A frequency control method for regulating wireless power to implantable devices. IEEE Trans. Biomed. Circuits Syst., 2: 22-29.

Sun, Y., X. Lv, Z. Wang and C. Tang, 2012. A quasi sliding mode output control for inductively coupled power transfer system. Inform. Technol. J., 11: 1744-1750.

Tang, C.S., Y. Sun, Y.G. Su, S.K. Nguang and A.P. Hu, 2009. Determining multiple Steady-state ZCS operating points of a Switch-mode contactless power transfer system. IEEE Trans. Power Electron., 24: 416-425.

Wang, C.S., G.A. Covic and O.H. Stielau, 2004. Power transfer capability and bifurcation phenomena of loosely coupled inductive power transfer systems. IEEE Trans. Ind. Electron., 51: 148-157.

Wang, Z.H., Y. Sun, Y.G. Su, X. Dai and C.S. Tang, 2010. A new type AC/DC/AC converter for contactless power transfer system. Trans. China Electrotech. Soc., 25: 84-89.

Wang, Z.H., Y. Sun, X. Dai and C.S. Tang, 2011. Design of converter of DC-AC type contactless power transfer system. J. Chongqing Univ., 34: 38-43.

Wu, H.H., G.A. Covic and J. Boys, 2011a. A low energy storage IPT system using AC processing controllers. Proceedings of the 6th IEEE Conference on Industrial Electronics and Applications, June 21-23, 2011, Beijing, China, pp: 351-356.

Wu, H.H., G.A. Covic, J.T. Boys and D.J. Robertson, 2011b. A series-tuned inductive-power-transfer pickup with a controllable AC-voltage output. IEEE Trans. Power Electron., 26: 98-109.

Zhang, L., Y. Sun, Z. Wang and C. Tang, 2013. Analysis of bifurcation phenomena of voltage-fed inductively coupled power transfer system varying with coupling coefficient. Inform. Technol. J., 12: 1176-1183.

Zheng, S.C., Q.Z. Zhou, X.H. Cao and H. Zhu, 2010. Principle of single phase AC/AC converter based on plugged pulse fashion and PWM control. Trans. China Electrotech. Soc., 25: 136-141.